Materials Letters 190 (2017) 225–228

Contents lists available at ScienceDirect

Materials Letters

journal homepage: www.elsevier.com/locate/mlblue

Ordered stacking faults within nanosized silicon precipitates in aluminum alloy

Dong Yue Xie [a], Jiawei Yan [a], Yangxin Li [a,b,*], Dong Qiu [c], Guilin Wu [d], Xiaodong Wang [a], Bin Chen [a], Yao Shen [a,*], Guo-zhen Zhu [a]

[a] State Key Laboratory of Metal Matrix Composites, School of Materials Science and Engineering, Shanghai Jiao Tong University, Shanghai 200240, PR China
[b] National Engineering Research Center of Light Alloy Net Forming, School of Materials Science and Engineering, Shanghai Jiao Tong University, Shanghai 200240, PR China
[c] School of Engineering, RMIT University, Carlton, VIC 3053, Australia
[d] College of Materials Science and Engineering, Chongqing University, Chongqing 400044, PR China

ARTICLE INFO

Article history:
Received 2 December 2016
Accepted 5 January 2017
Available online 6 January 2017

Keywords:
Aluminum alloys
Precipitation
Ordered stacking faults
Interfaces
Electron microscopy

ABSTRACT

A considerable amount of superfine Si precipitates with the sizes ranging from 5 to 15 nm were found uniformly dispersed in the Al matrix of an Al-1Si (wt.%) alloy after electropulsing treatment. Through high resolution transmission electron microscopy (HRTEM), an unusual 9R (*ABCBCACAB*...) ordered stacking faults were identified within the Si precipitates with a truncated tetrahedral morphology that hold a $(1\,1\,1)_{Si}//(1\,1\,1)_{Al}$ & $[1\,0\,\bar{1}]_{Si}//[1\,\bar{1}\,0]_{Al}$ orientation relationship with the Al matrix. An atomistic model was established to preform image simulations and explain that the existence of these nanosized Si precipitates is attributable to increment of coincidence lattice sites between Si and Al.

1. Introduction

Al-Si alloys have been widely used in modern automotive and aerospace industries because they usually exhibit an excellent combination of low-density, high-strength, and wear-resistance [1–3]. However, coarse Si particles were usually found, decreasing the strength of most Al-Si alloys. The precipitation of silicon from supersaturated aluminum solid solution is a common strategy to obtain superfine silicon precipitates, which plays a significant role in strengthening Al-Si alloys [4–6].

Electropulsing treatment is a novel approach of energy input assisted processing technology in order to refine grains, improve mechanical properties and influence phase transformation, by means of acceleration of atomic diffusion and decrease of thermodynamic barrier [7,8]. In this paper, we report the refinement of Si precipitates in Al-Si alloys by electropulsing treatment, focusing on morphological features of the nanosized Si precipitates and their forming mechanism.

2. Materials and methods

Alloy with chemical composition of Al-1Si (wt.%) was cast from 99.999% purity Al and high purity Si. After solution treatment at 570 °C for 12 h, the alloy was ethanol-quenched to −30 °C for 2 h. Electropulsing treatment was then applied to the samples for 3–10 s to obtain Si precipitates in the Al matrix at ambient temperature. The duty ratio, the maximum electric current density, and the frequency are 1:32, 1500 A/mm^2 and 58 Hz for the electric pulses, respectively. TEM specimens were prepared using two-jet polishing and ion-milling techniques, then were characterized in a JEOL JEM-ARM200F microscope operating at 200 kV. The HRTEM multislice image simulation, based on proposed atomic models with different specimen thicknesses, was performed by JEMS software, under varying defocus conditions from −50 to 50 nm with 10 nm intervals.

3. Results and discussion

As shown in a typical TEM bright-field image of the electropulsing treated Al-Si alloy in Fig. 1a, a great number of nanosized precipitates with 5–15 nm in size are uniformly dispersed in the Al matrix. The interspacing between precipitates is about 50–100 nm. Most precipitates have a polyhedral morphology. In

* Corresponding authors at: State Key Laboratory of Metal Matrix Composites/National Engineering Research Center of Light Alloy Net Forming, School of Materials Science and Engineering, Shanghai Jiao Tong University, Shanghai 200240, PR China.
E-mail addresses: astatium@sjtu.edu.cn (Y. Li), yaoshen@sjtu.edu.cn (Y. Shen).

http://dx.doi.org/10.1016/j.matlet.2017.01.023
0167-577X/

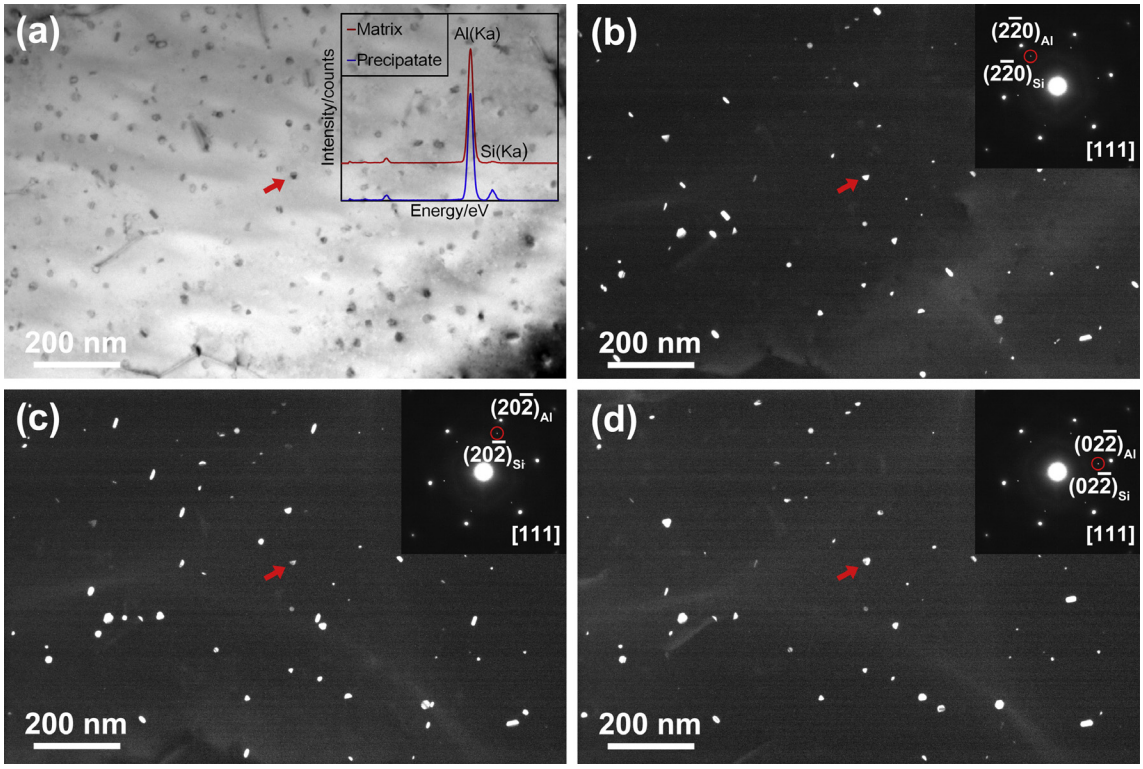

Fig. 1. (a) TEM-BF image of electropulsing treated Al-1Si alloy with inset EDX spectra; (b)-(d) $\{220\}_{Si}$ CDF images, showing the existence of a $(111)_{Si}//(111)_{Al}$ & $[10\bar{1}]_{Si}//[1\bar{1}0]_{Al}$ orientation relationship.

particular, some precipitates exhibit a truncated tetrahedral morphology and the projections of them always have a triangular shape. According to the Al-Si binary phase diagram [9], these precipitates were expected to be silicon, which were confirmed by the Energy dispersive X-ray (EDX) spectrum (Fig. 1a). These precipitates remain a silicon lattice structure, with their SAED patterns inset in Fig. 1(b-d). Viewed from $[111]_{Al}$ (Fig. 1), weak reflections with sixfold symmetry are indexed as the $\{220\}_{Si}$, located inside the $\{220\}_{Al}$ reflections. The reflections from those precipitates are isolated weak spots instead of concentric rings for randomly oriented precipitates, indicating the existence of ORs with the Al matrix. The centered dark-field (CDF) images from selected $\{220\}_{Si}$ reflections, marked by red circles in the insets of SAED patterns in Fig. 1(b-d), additionally indicate different oriented precipitates with respect to the matrix, which are evenly distributed within the Al matrix.

Statistical study of over a few hundred precipitates shows that about 10% precipitates are triangular-shaped, holding a $(111)_{Si}//(111)_{Al}$ & $[10\bar{1}]_{Si}//[1\bar{1}0]_{Al}$ OR with the Al matrix. Similar OR was previously observed in Al–Si [10], Al–Si–Ge [11], Al–Si–Ge–Cu [12] alloys and deposited Al layer on Si wafer [13]. One triangular-shaped precipitate (the red arrow in Fig. 1) was enlarged to study its three-dimensional morphology. When viewed along $[111]_{Al}$ in Fig. 2a, none facets of this precipitate presents sharp interface. After tilted to $[112]_{Al}$, the left-hand side facet was at edge-on condition and parallel to the $(11\bar{1})$ plane, as shown in Fig. 2b. Therefore, it is reasonable to deduce that such tetrahedral Si precipitates have four equivalent major facets parallel to $\{111\}_{Si}$ and $\{111\}_{Al}$ planes.

Since Al and Si have a significant difference in their lattice constants (a_{Al} = 0.4050 nm, a_{Si} = 0.5431 nm), it is impossible for Si precipitates to hold a coherent or even semi-coherent interface with Al matrix at an $\{111\}_{Si}//\{111\}_{Al}$ interface. However, given that $4a_{Al} \approx 3a_{Si}$, the $\{111\}_{Si}//\{111\}_{Al}$ interface becomes commensurable when $<1\bar{1}0>_{Si}//<1\bar{1}0>_{Al}$. If we force the lattice constants to be $4a_{Al\text{-}C} = 3a_{Si\text{-}C}$ (subscript 'C' means constraint), a constraint coincidence site lattice (CCSL) can be established between Si and Al. If this constraint to the Al lattice is removed, a small secondary lattice misfit can be defined as $\delta = (3a_{Si} - 4a_{Al})/(4a_{Al}) = 0.58\%$. Accordingly, we can determine the resultant spacing of the secondary misfit dislocations $D_{disl} = |b^{II}|/\delta = (1/4^{*}a_{Si\text{-}C})/\delta = (1/3^{*}a_{Al\text{-}C})/\delta = 16.6$ nm, where b^{II} is the Burgers vector of the constrained complete pattern shift lattice (DSCL) [14]. Since the size of tetrahedral precipitates is 5–15 nm, which is just less than the spacing of the secondary misfit dislocations, these Si precipitates still hold the CCSL interface with their Al matrix while the local Al atoms close to the interface can bear such small tension without introducing secondary misfit dislocations. This is consistent with our HRTEM observations as no misfit dislocation was identified around the interface.

We recorded diffuse spots and streaks over 20 triangular-shaped precipitates under different zone axes (Fig. 2(b-d)), indicating the possible existence of stacking faults [15–19]. These features are similar to those from a 9R stacking sequence (*ABCBCACAB*...) reported in the literature [15,17]. Accordingly, we proposed an atomistic model of such a 9R stacking sequence (Fig. 2e). The simulated SAED pattern from our model (Fig. 2f) has a nearly perfect agreement with the detected FFT pattern in Fig. 2c and a fairly good agreement with the experimental SAED pattern (Fig. 2d) although some spots are missing due to their poor detectability. These red-circled reflections can only be formed by the diffraction of 9R stacking faults. To isolate the contribution of 9R stacking faults to such periodic contrast in HRTEM image, atomic models, which contain Si with or without such 9R stacking faults sand-